Expanding the clinical phenotypes of *MT-ATP6* mutations

Ester López-Gallardo[1,6], Sonia Emperador[1,6], Abelardo Solano[1], Laura Llobet[1,6],
Antonio Martín-Navarro[1], Manuel José López-Pérez[1,6], Paz Briones[3,6], Mercedes Pineda[4,6],
Rafael Artuch[5,6], Elena Barraquer[7], Ivonne Jericó[8], Eduardo Ruiz-Pesini[1,2,6] and Julio Montoya[1,6,]*

[1]Departamento de Bioquímica, Biología Molecular y Celular, Instituto de Investigación Sanitaria de Aragón, Zaragoza, Spain, [2]Fundación ARAID, Universidad de Zaragoza, 50013 Zaragoza, Spain, [3]Servicio de Bioquímica y Genética Molecular, Hospital Clínico, IDIBAPS, 08036-Barcelona, Spain, [4]Servicio de Neurología and [5]Departamento de Bioquímica Clínica, Hospital San Joan de Deu, 08950 Barcelona, Spain, [6]Centro de Investigaciones Biomédicas en red de Enfermedades Raras (CIBERER), Spain, [7]Clínica Barraquer, 08021 Barcelona, Spain and [8]Servicio de Neurología, Complejo Universitario de Navarra, 31008-Pamplona, Spain

Mitochondrial DNA mutations at *MT-ATP6* gene are relatively common in individuals suffering from striatal necrosis syndromes. These patients usually do not show apparent histochemical and/or biochemical signs of oxidative phosphorylation dysfunction. Because of this, *MT-ATP6* is not typically analyzed in many other mitochondrial disorders that have not been previously associated to mutations in this gene. To correct this bias, we have performed a screening of the *MT-ATP6* gene in a large collection of patients suspected of suffering different mitochondrial DNA (mtDNA) disorders. In three cases, biochemical, molecular-genetics and other analyses in patient tissues and cybrids were also carried out. We found three new pathologic mutations. Two of them in patients showing phenotypes that have not been commonly associated to mutations in the *MT-ATP6* gene. These results remark the importance of sequencing the *MT-ATP6* gene in patients with striatal necrosis syndromes, but also within other mitochondrial pathologies. This gene should be sequenced at least in all those patients suspected of suffering an mtDNA disorder disclosing normal results for histochemical and biochemical analyses of respiratory chain.

INTRODUCTION

Approximately 10–20% of individuals with Leigh syndrome (LS) and more than 50% of individuals with neurogenic muscle weakness, ataxia and retinitis pigmentosa (NARP) have a mutation at mitochondrial DNA (mtDNA) nucleotide position 8993 of the *MT-ATP6* gene (1). These two clinical conditions have been termed 'striatal necrosis syndromes' and have been also associated to mutations at nucleotide position 9176 of the *MT-ATP6* gene (2). Thus, these mutations have been frequently analyzed in persons suffering these pathologies. In these patients, histologic examination of muscle biopsies shows only minimal, if any, changes and the specific activities of respiratory complexes are usually normal (1), because the p.MT-ATP6 polypeptide is not a component of the respiratory

chain but of the oxidative phosphorylation system (OXPHOS) complex V (CV) or ATP synthase. Moreover, for ADP phosphorylation to take place, mitochondria need to be maintained intact and in a coupled state. Then, ATP synthesis can only be measured on freshly isolated mitochondria (3). Therefore, ATP synthase-specific activity is not regularly measured in patients' tissues. Because of the general lack of positive histochemical and biochemical evidences on the implication of p.MT-ATP6 in a particular pathology based in *MT-ATP6* mutations, its screening in other mitochondrial diseases has been infrequent.

To avoid these biases, we have performed a screening of the *MT-ATP6* gene in a big collection of patients suspected of suffering mtDNA disorders, as NARP, maternally inherited LS (MILS) and other with very different clinical phenotypes.

*To whom correspondence should be addressed at: Departamento de Bioquímica, Biología Molecular y Celular, Universidad de Zaragoza, C/ Miguel Servet, 177, 50013 Zaragoza, Spain. Tel: +34 976761640; Fax: +34 976761612; Email: jmontoya@unizar.es

RESULTS

MT-ATP6 analysis

Three out of the 550 patients studied harbored interesting mutations in their *MT-ATP6* genes. These mutations consisted of transitions at m.9025G>A, m.9029A>G and m.9032T>C nucleotide positions for P1, P2 and P3, respectively (Fig. 1). To rule out the presence of other potentially pathological mutations, we sequenced the complete mtDNAs of these three patients, but no other variant was a better candidate for being the pathogenic mutation (Supplementary Material, Note S1). These analyses also provided us their mtDNA haplogroups (U5b2b3, W1* and U5b1f). Next, we analyzed the presence of these mutations in 21 580 human p.MT-ATP6 sequences obtained from GenBank plus 4352 from different publications (Supplementary Material, References S1). The m.9025G>A, m.9029A>G and m.9032T>C transitions were found 13, 1 and 0 times, respectively, in apparently healthy individuals and always in different mtDNA genetic backgrounds and distinct from our patients (Supplementary Material, Note S2). To rule out these mutations as more geographically restricted polymorphisms, we also studied 13 and 18 Spaniard population samples from mtDNA haplogroups W and U5b, respectively. The mutations were not found in any of them. In addition of the 550 patients from the initial screening, we also analyzed by real-time polymerase chain reaction (PCR) the m.9025G>A/ m.9032T>C and m.9029A>G transitions in all remaining samples of our laboratory from individuals suspected of suffering from MILS/NARP and optic neuropathy, respectively. We found the m.9025G>A mutation in a MILS patient (P4, Supplementary Material, Note S1). Finally, the m.9025G>A mutation had been found in one patient with colon cancer from haplogroup H7d3a and another with motor neuropathy and the m.9029A>G transition had also been found in one patient from haplogroup H with suspected mitochondrial disorder (Supplementary Material, References S2).

These mutations were firstly discovered by conformation sensitive gel electrophoresis (CSGE) and/or sequencing (Supplementary Material, Fig. S1A). To rule out sequencing artifacts and confirm the presence of these mutations by another different method, we performed PCR-restriction fragment length polymorphism (RFLP) analyses. These mutations were found in heteroplasmy in at least one individual from each pedigree (Supplementary Material, Fig. S1B). However, the mtDNA region around these mutations is highly represented in nuclear mitochondrial DNA sequences (NUMTs) (4) and short amplicons for m.9025G>A and m.9029A>G, but not for 9032T>C, analyses were observed from rho[0] cells (Supplementary Material, Fig. S1C). Therefore, to ratify heteroplasmies, determine their true percentages and their association with the phenotype, we designed a larger amplicon (Supplementary Material, Fig. S1D) and performed a nesting radioactive PCR-RFLP in probands and relatives. The m.9025G>A mutation was found in homoplasmy in proband's muscle, liver and blood and in mother's and sister's blood (Fig. 2A). The m.9029A>G mutation was found in homoplasmy in the patient's blood but in heteroplasmy in his mother (95%) and siblings (brother 85%, sister 95%) (Fig. 2B). This heteroplasmy is authentic because only two NUMTs in chromosomes 5 and 17 have enough length to be amplified with our PCR conditions and, despite that their targets for the
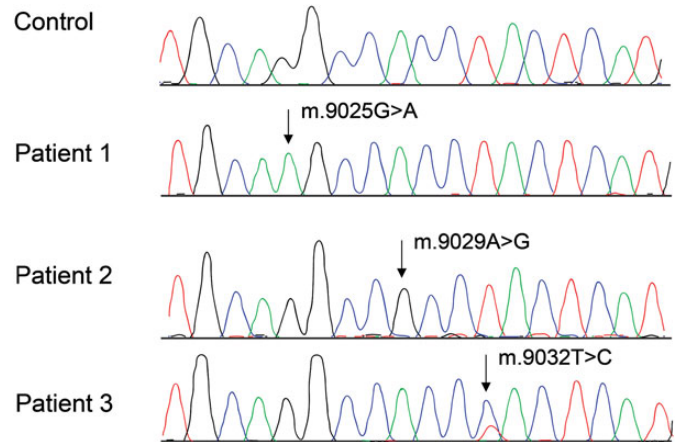

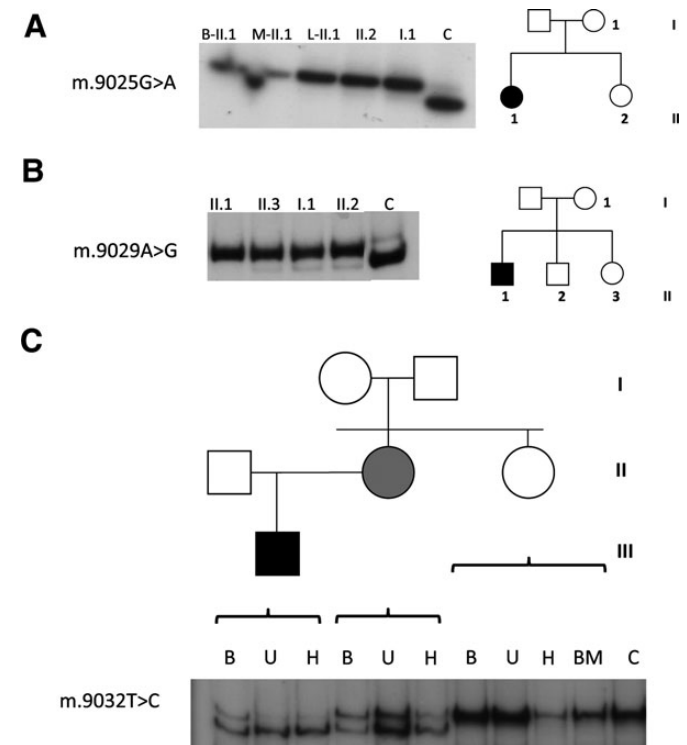**Figure 1.** Electropherograms from segments of the *MT-ATP6* gene. Heteroplasmy at m.9032 position can be observed.

Figure 2. Hot PCR-RFLP. (**A**) m.9025G>A transition. C, B, L, M, I and II denote control, blood, liver, muscle, first and second generation, respectively. Black and white figures represent the patient and non-affected relatives, respectively. (**B**) m.9029A>G transition. C, I and II denote control, first and second generation, respectively. Black and white figures represent the patient and non-affected relatives, respectively. (**C**) m.9032T>C transition. C, B, BM, H, U, I, II and III denote control, blood, buccal mucosa, hair, urine, first, second and third generation, respectively. Black, grey and white figures represent the patient, the moderately affected mother and other non-affected relatives, respectively.

genotyping restriction enzyme are identical to that of the normal mtDNA sequence, there are many mispairings in the primers-matched sequences (Supplementary Material, Note S3) and this segment was not amplified in rho[0] cells (Supplementary Material, Fig. S1D) or the patient blood (Fig. 2B). The m.9032T>C
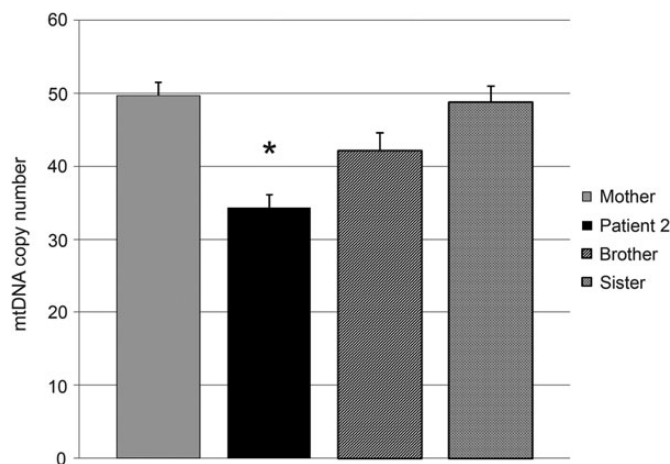
Figure 3. mtDNA levels in members of the m.9029A>G pedigree. The asterisk denotes significant differences ($P \leq 0.0078$) from the rest of pedigree members.

transition was found in heteroplasmy in proband's urine (96%), hair (93%) and blood (70%) and also in mother's hair (73%), urine (57%) and blood (42%) but it was not found in hair, urine, buccal mucosa or blood of a healthy maternal aunt (Fig. 2C).

As the mutation m.9025G>A was found in homoplasmy in the asymptomatic mother and sister and m.9029A>G was found at a high percentage in the asymptomatic mother and siblings, we looked for potential compensatory factors, such as the mtDNA levels, in symptomatic and asymptomatic family members (5). There were no differences in mtDNA levels in members of the m.9025G>A pedigree, but they were significantly lower in the m.9029A>G patient than in his relatives (Fig. 3).

P.MT-ATP6 analysis

The m.9025G>A, m.9029A>G and m.9032T>C transitions provoke glycine to serine, histidine to arginine and leucine to proline amino acid substitutions, respectively. The MutPred score mean $\pm$ standard deviation for all of the 24 206 possible amino acid variations defined by a single point mutation away from the revised Cambridge reference sequence (rCRS) is 0.642 ± 0.154 (6). These values for all of the 111 glycine to serine, 97 histidine to arginine and 553 leucine to proline possible substitutions were 0.749 ± 0.120, 0.728 ± 0.166 and 0.737 ± 0.105, respectively, and they were significantly higher than those for all of the possible amino acid substitutions ($P < 0.0001$). The particular values for these changes were 0.860 (G167S), 0.827 (H168R) and 0.837 (L169P) (Table 1). Because a higher pathogenicity score correspond to a greater likelihood that the amino acid variation is pathogenic, these results suggest that these particular amino acid substitutions will have phenotypic consequences.

The G167, H168 and L169 amino acids are extremely preserved through evolution. Thus, they were conserved in 99.7, 98.1 and 87.9%, respectively, of 3410 published p.MT-ATP6 reference sequences from animals, plants, fungi and protists (Table 1). G167 was the second most conserved p.MT-ATP6 position after R159, a key residue for proton transport. As there is a bias in the type of organisms with their mtDNAs sequenced

(most of the sequenced mtDNAs belong to animals), to confirm the clues about the functional importance of these amino acids, we also estimated the conservation indexes (CI) for these positions in 1409 bacteria that are organisms very distant from an evolutionary point of view. The CIs were 86.2, 36.0 and 33.4%, respectively (Table 1).

The G167, H168 and L169 amino acids are located in the transmembrane helix 4 (TMH4) of p.MT-ATP6 (Fig. 4A and B). TMH4 and TMH5 of p.MT-ATP6 and TMH2 of subunit c form the F1F0 ATP synthase proton channel (7). Four other positions affected by pathologic mutations (A155, L156, A162 and L170) are also located in this TMH4. Moreover, G167 and L169 are placed along with A155, L156, R159, A162 and L170 in the most conserved side of TMH4 (Fig. 4C). A structurally compensating replacement in any of these TMHs could explain the phenotypic differences between the homoplasmic m.9025G>A patient and her asymptomatic maternal relatives. However, there were not differences between the p.MT-ATP6 and c subunits (the three isoenzymes) from the patient and relatives.

Cybrid analysis

The previous results suggested that these mutations might be functionally important and, maybe, they were responsible for patients' phenotypes. To confirm this possibility, we built seven transmitochondrial cell lines (cytoplasmic hybrids or cybrids) using the osteosarcoma 143B206 rho^0 cell line as the common nuclear background (8) and platelets from each of these patients. Unfortunately, family of deceased P1 did not want to continue with the study and from P4, a patient studied 7 years ago, we only had muscle. Therefore, we could not produce cybrids with this mtDNA mutation. We used a haplogroup H cybrid harboring the homoplasmic m.8993T>G pathologic mutation as a positive control. As negative controls, we used the isogenic m.8993T cybrid and, as it has been previously shown that the mtDNA genetic background plays an important role in modulating the biochemical defects and clinical outcome in NARP/MILS (9), we also generated cybrids from healthy individuals from close haplogroups to those of the patients. Thus, H, N1b and Uk cybrids were negative controls (C5, C2 and C3) for mutant H, W1* and U5b cybrids (P5, P2 and P3), respectively.

First, we confirmed that the cybrids harbored the nuclear background of osteosarcoma 143B206 rho^0 cells and the mtDNA of the donor platelets (Supplementary Material, Fig. S2).

Compared with their haplogroup controls, mutant cybrids harboring the homoplasmic m.8993T>G, m.9029A>G and heteroplasmic (25 and 80%) m.9032T>C mutations presented a decrease in the endogenous oxygen consumption (Fig. 5A), but there were no differences in leaking respiration (Fig. 5A). Uncoupled respiration was not different from control cybrids in m.8993T>G and m.9029A>G cybrids but was significantly lower in m.9032T>C cybrids (Fig. 5A).

The mitochondrial inner membrane potential was significantly lower in the m.8993T>G cybrid than in its haplogroup control cybrid. However, this parameter was significantly higher in m.9029A>G and m.9032T>C (25%) cybrids than in their controls (Fig. 5B). This potential was not different from that of the haplogroup control in the m.9032T>C (80%) cybrid (Fig. 5B).

Table 1. Pathologic mutations in the *MT-ATP6* gene

p.MT-ATP6 *MT-ATP6*	Mutation load	Phenotype	Pathologic pedigrees	Controls (>25 000)	Mt-CI (%) (3410)	B-CI (%) (1409)	MutPred	Cybrids
Previously reported mutations								
p.M1T m.8528T>C	Ho−He	IC	S	0	69.8	–	0.983	N
p.A105P m.8839G>C	He	NARP	O	0	80.9	–	0.742	C
p.W109R m.8851T>C	Ho−He	BSN	S	1	90.9	–	0.780	N
p.A155P m.8989G>C	He	NARP	O	0	67.6	13.3	0.742	N
p.L156P/R m.8993T>C/G	He/He	AOSA/NARP/LS	S/S	0/0	99.1	84.0	0.846/0.824	C/C
p.A162V m.9011C>T	Ho	LHON	O	1	95.0	30.5	0.728	C
p.L170P m.9035T>C	Ho−He	Ataxia/AOSA	S	0	91.0	23.0	0.865	C
p.L217P/R m.9176T>C/G	He/He	LS	S/S	1/0	98.4	96.5	0.719/0.777	C/C
p.L220P m.9185T>C	Ho−He	AOSA/NARP/LS/CMT	S	0	86.8	11.1	0.751	N
p.L222P m.9191T>C	He	LS	O	0	72.7	38.2	0.844	N
New mutations								
p.G167S m.9025G>A	Ho	CC, MN, LS-like	S	13	99.7	86.2	0.860	N
p.H168R m.9029A>G	Ho−He	LHON-like	S	1	98.1	36.0	0.827	C
p.L169P m.9032T>C	He	NARP	O	0	87.9	33.4	0.837	C

To consider a previously published p.MT-ATP6 mutation as a pathologic one, the mutation should fulfill at least one of these two criteria: (i) the mutation should be present in more than one pathologic pedigree, its population frequency should be very low (below 0.05%) and it should not be located at internal branches of the mtDNA phylogenetic tree or (ii) phenotypic differences should be shown between cell models harboring different percentages of mutant and control mtDNAs. The m.8989G>C and m.9191T>C mutations do not fulfill these criteria. However, several other features suggest that they are pathologic mutations. AOSA, adult-onset spinocerebellar ataxia; B-CI, conservation index for bacterial subunit a; BSN, bilateral striatal necrosis; C, cybrids; CC, colon cancer; CMT, Charcot-Marie-Tooth; Ho, homoplasmy; He, heteroplasmy; IC, infantile cardiomyopathy; LHON, Leber hereditary optic neuropathy; LS, Leigh syndrome; MN, motor neuropathy; Mt-CI, conservation index for p.MT-ATP6; MutPred, a proxy index for the pathogenicity of an amino acid variation (6); N, No; NARP, neuropathy, ataxia and retinitis pigmentosa; O, one; S, several. A hyphen in the B-CI column signifies that we cannot trustworthily indicate the equivalent amino acid in the bacterial subunit a.

ATP levels in mutant cybrids were lower than those of their control cybrids (Fig. 5C), except for the m.9032T>C (25%) cybrid.

Reactive oxygen species (ROS) and Mn superoxide dismutase (SOD2) mRNA levels in mutant cybrids were also significantly higher than those of their control cybrids, except for the m.9032T>C (25%) cybrid (Fig. 5D).

Therefore, when compared with normal mtDNAs, the relocation of these mutated mtDNAs to rho^0 cell lines transfers altered biochemical features.

DISCUSSION

M.9025G>A associated with type IV 3-methylglutaconic aciduria

The m.9025G>A/p.MT-ATP6:G167S mutation fulfills some but fails in other of the accepted pathogenicity criteria. Thus, this mutation was found in homoplasmy in healthy relatives and, except for Leber hereditary optic neuropathy (LHON) and mitochondrial deafness, this is not a common observation in disorders due to mtDNA mutations. However, the homoplasmic m.9176T>C/p.MT-ATP6:L217P mutation has also been associated with a very mild disease course in some individuals from two pedigrees suffering hereditary spastic paraplegia-like disorder (10) and Charcot-Marie-Tooth hereditary neuropathy (11). Homoplasmic levels of the m.9185T>C/p.MT-ATP6:L220P mutation were found in several slightly affected individuals from another pathologic pedigree (12). The m.9025G>A mutation has been found in 13 out of more than 25 000 (0.05%) apparently healthy individuals, but all of them from different mtDNA genetic backgrounds, which means that this is not an ancient polymorphism. Moreover, other *MT-ATP6* pathologic mutations, such as m.8851T>C/p.MT-ATP6:W109R, m.9011C>T/p.MT-ATP6:A162V and m.9176T>C/p.MT-ATP6:L217P, have been found in homoplasmy in individuals from different population studies (Supplementary Material, Note S2). In all these examples, other factors such as nuclear modifying genes, the mtDNA genetic background or environmental influences may be involved in determining the severity of the phenotypic expression and the large phenotypic variability of these *MT-ATP6* mutations (10). On the other hand, G167 is the second most conserved amino acid position in the p.MT-ATP6 subunit and bioinformatics studies predict that the glycine to serine amino acid substitution at p.MT-ATP6 167 position would be pathologic (6).

The glycine of the equivalent position in bacteria is also extremely conserved (86.2% of 1409 bacteria species). Many bacteria lacking a glycine in this position have a glycine at the
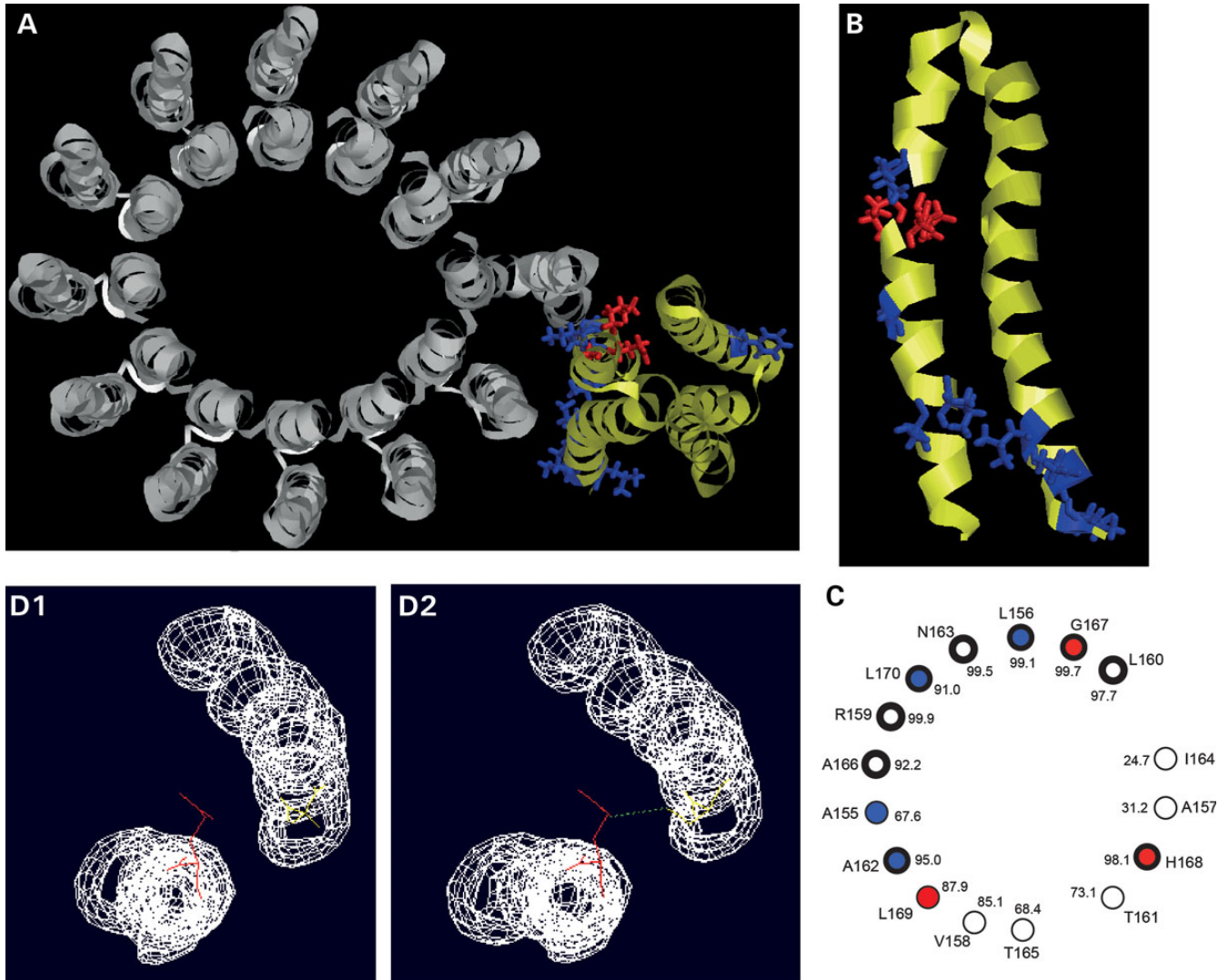
Figure 4. The molecular model of the p.MT-ATP6 subunit. (**A**) View of subunit a (yellow color) (the bacterial orthologue of mitochondrial p.MT-ATP6) and subunits c (grey color) of *Escherichia coli* from the periplasma (intermembrane) space. The bacterial equivalent p.MT-ATP6 positions that, when mutated, have been associated to human disorders (blue color) have been represented in this model. New mutations described in this article are represented in red color. (**B**) p.MT-ATP6 TMH4 and TMH5. Already described and newly described pathologic mutations are represented in blue and red color, respectively. (**C**) Helical wheel representation of TMH4. Pathologic positions are represented with blue and red circles and those with a CI > 90% with thick lines. (**D**) G167 (yellow color), in TMH4, does not interact with E203 (red color) of TMH5 (D_1) but S167 (yellow color) establishes a hydrogen bond (green line) with E203 (red color) of TMH5 (D_2).

equivalent position to amino acid 203 in TMH5 that interacts with amino acid at position 167 in TMH4 (2). Thus, glycine is frequently a member of the interacting amino acid pair. This pair forms part of an aqueous pocket extending from D61 of subunit c to the periplasmic surface (13). Glycine is the smallest amino acid and the bigger hydrophilic S167 might form a hydrogen bond with the E203 (Fig. 4D) and alter the conformational movements of this helix (14). Also supporting an important role of this amino acid position, the ATP synthase of extreme alkaliphiles has special features that are required for non-fermentative growth and OXPHOS at high pH ($\geq$10.5). At such pH values, maintenance of a cytoplasmic pH that is acid in, lowers the total chemiosmotic driving force, and yet a robust H^+-coupled OXPHOS proceeds optimally. The K180 amino acid of these alkaliphilic bacteria (amino acid position 167 in humans) is implicated in the pH-dependent restriction

of the proton flux through the ATP synthase to and from the bulk phase (15). Moreover, different replacements at the equivalent position to human 167 have been modeled in *E. coli* and the ATP synthase activity was greatly inhibited and the aerobic growth suppressed. Replacing this amino acid by a polar one caused proton leak (14,16–18).

All these forward and against evidences on the pathogenicity of this mutation prevent its assignation as a pathologic change and make necessary more proofs.

The clinical phenotype and the increased levels of 3-methylglutaconic acid in our patient suggested a type IV 3-methylglutaconic aciduria. This is a mixed bag diagnostic but, frequently, a defect on the OXPHOS system has been found for these patients (Supplementary Material, References S3). Our results allowed us to rule out a defect of respiratory complexes, a coenzyme Q (CoQ) deficiency or an mtDNA
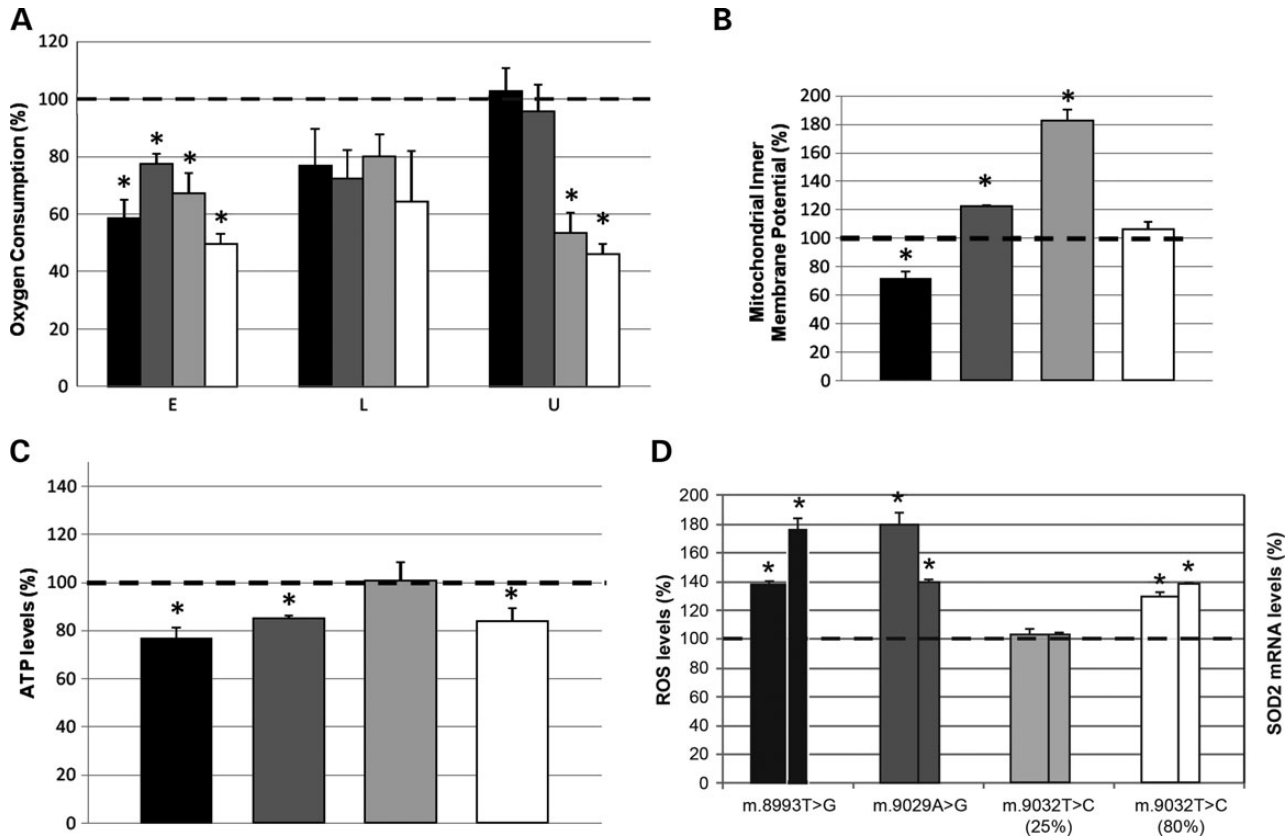
Figure 5. Biochemical characterization of the cybrid cell lines. Black, dark gray, light gray and white code for m.8993T>G, m.9029A>G, m.9032T>C (25%) and (80%) cybrids, respectively. Asterisks denote significant differences ($P \leq 0.0074$). (**A**) Oxygen consumption. E, L and U code for endogenous, leaking and uncoupled oxygen consumption. (**B**) Mitochondrial inner membrane potential. (**C**) ATP levels. (**D**) ROS quantity and SOD2 mRNA expression. Wide and strait bars code for ROS and SOD2 mRNA levels, respectively.

deletion or depletion. The 3-methylglutaconic aciduria has sometimes been found in LS, but we were able to rule out several causes of LS such as pyruvate dehydrogenase (PDH) complex deficiency. LS caused by *MT-ATP6* mutations frequently show normal activities for the electron transport chain complexes such as those found in our patient. Moreover, 3-methylglutaconic aciduria is frequently found in ATP synthase deficiency and, particularly interesting, it was found in a patient with the pathologic mutation m.8993T>G in the *MT-ATP6* gene.

M.9029A>G associated with atypical LHON

The m.9029A>G/p.MT-ATP6:H168R mutation fulfills most of the accepted pathogenicity criteria. However, this mutation was also reported in two other individuals out of more than 25 000 including patients and controls. This observation is not rare for mtDNA mutations associated to hereditary optic neuropathies. Thus, the m.11778G>A and m.14484T>C transitions are frequently found in homoplasmy in normal females of LHON pedigrees. Moreover, two individuals without evidence of visual abnormalities and not being part of LHON families harbored these homoplasmic LHON pathogenic mutations (19). More importantly, one of these two individuals with the m.9029A>G mutation was suspected of suffering a mitochondrial disorder (20). On the other hand, and supporting its pathogenic role, this mutation is also the best candidate mutation to explain a

pathologic phenotype (optic neuropathy) frequently found associated to pathologic mtDNA mutations. It was in homoplasmy in the proband and in heteroplasmy in the unaffected relatives. Despite the percentage of heteroplasmy was very high in the healthy relatives, maybe their higher mtDNA content may contribute to a moderate amount of normal mtDNA genotypes that compensate the pathologic mutation (21). The mutation changes a highly conserved amino acid in an important transmembrane alpha-helix which is part of the ATP synthase proton channel. Moreover, 3 (W109R, L156R and L217R) out of 12 previously described *MT-ATP6* pathologic mutations incorporate an arginine. Finally, the m.9029A>G cybrid show OXPHOS dysfunction when compared with the cybrid harboring a normal mtDNA genotype from a close mtDNA haplogroup.

By using the Ag$^+$-chemical labeling of cysteine side chains, introduced by site-directed mutagenesis, to map the aqueous accessible regions on subunit a (bacterial ortologue of mitochondrial p.MT-ATP6), it was found that the bacterial equivalent position to amino acid 168 might be part of an aqueous pathway to the intermembrane space (13). Moreover, it has been proposed that the proton motive force causes protonation of a network of residues in subunit a near the intermembrane surface, including amino acid 168 (22,23). Therefore, the H168R substitution, with very different pK, should have an important phenotypic effect. Interestingly, different amino acid replacements have been modeled at this equivalent position

in *E. coli* (corresponding to position 219), showing that the proton translocation and the ATP synthase activity was greatly inhibited, and that the aerobic growth was also affected (16,24–27).

The main interest of m.9029A>G is that it is associated with an atypical LHON phenotype. Many patients are not fully evaluated early in the course of the disease or are referred electively for a subspecialty opinion years later. Properly evaluating an individual with suspected optic neuropathy years after the visual loss occurred may be difficult (28). Sometimes, rare optic neuropathies in patients harboring common LHON mutations can be confused with ischemic optic neuropathy (29,30), as it was the case of this patient. Moreover, LHON progression varies considerably, ranging from sudden and complete vision loss to progressive decline up to 2 years (31). However, the progressive loss of vision in our patient over 4 years, although highly unusual, has already been reported in an individual with the m.11778G>A pathologic mutation (32).

It is considered that LHON is caused by mutations in mtDNA-encoded complex I subunits. Mutations in *MT-ND* genes have been associated to LHON but also to LS. Moreover, some LHON mutations have been sometimes associated to LS (33). Therefore, it would be possible that *MT-ATP6* mutations, usually associated to LS, were etiologic factors for LHON. A lowered rate of oxidative ATP synthesis appears to be the common biochemical background of pathogenic importance in all LHON complex I mutations (34). This background is also accompanied by an increased ROS production (35). The p.MT-ATP6 mutations that cause LS also reduce the ATP production (36) and increase ROS production (37). Very interestingly, the few histopathological studies reporting ocular findings in LS patients indicate that these individuals show features indistinguishable from LHON (38,39). Thus, maybe LHON is not a defect of mtDNA-encoded complex I subunits but of mtDNA-encoded OXPHOS subunits. Our results on ROS and ATP levels from cybrids harboring the m.9029A>G transition show that, in addition to *MT-ND* mutations, other mtDNA mutations could be associated to hereditary optic neuropathies. In fact, and although nowadays evidences are not too strong, other *MT-ATP6* mutations, such as m.9101T>C/ p.MT-ATP6:I192T (40) and m.9011C>T/p.MT-ATP6:A162V (41) have been postulated as etiologic factors for LHON patients. The m.9101T>C transition induced a proton leak that reduced OXPHOS efficiency (40) and this phenotype was transferred to cybrids (42). Moreover, cybrids harboring the m.9011C>T transition showed decreased calcium levels (43).

M.9032T>C associated with NARP

The m.9032T>C/p.MT-ATP6:L169P mutation fulfills all the accepted pathogenicity criteria. It was the best mtDNA candidate mutation to explain a pathologic phenotype (NARP) frequently found associated to pathologic mutations in the *MT-ATP6* gene. It has not been found in normal individuals. It is present in heteroplasmy in the affected individuals, but it was not present in a healthy relative. It changes a highly conserved amino acid in an important transmembrane alpha-helix which is part of the ATP synthase proton channel. This mutation incorporates the same amino acid than other pathologic mutations of the same subunit, such as A105P, A155P, L156P, L170P, L217P, L220P and L222P, also associated to NARP/MILS phenotypes. A proline inside a transmembrane alpha-helix provokes the loss of hydrogen

bonds in the peptide bonds, destabilizes the secondary structure and introduces a kink in the alpha-helix (44,45). Finally, cybrids harboring mutant mtDNA genotypes show OXPHOS dysfunction when compared with the cybrid harboring a normal mtDNA genotype from the same mtDNA haplogroup.

CONCLUSIONS

Our results on P3 patient (m.9032T>C) remark the importance of sequencing the entire *MT-ATP6* gene in NARP/MILS patients. These analyses are providing new pathologic mutations, such as m.8618-8619insT (46), m.8839G>C (47) or m.8989G>C (48), as etiologic factors for these syndromes. Recent results also suggest that *MT-ATP6* sequencing in other mitochondrial pathologies, no previously associated to *MT-ATP6* mutations, unmask already known pathologic mutations as responsible for these clinical conditions, such as m.9185T>C in the Charcot-Marie-Tooth disease (49) or in the episodic weakness (50). Finally, these studies are also revealing new *MT-ATP6* mutations in other mitochondrial disorders, such as m.8528T>C in infantile cardiomyopathy (51) or m.9025G>A and m.9029A>G in 3-methylglutaconic aciduria and hereditary optic neuropathy, respectively (this study). To increase the success rate in the finding of *MT-ATP6* pathologic mutations, this gene should be sequenced at least in those patients suspected of suffering a mtDNA disorder and negatives for histochemical and biochemical analyses of respiratory chain defects. However, a positive marker is still required to improve the diagnostic efficiency of p.MT-ATP6 defects. Maybe, 3-methylglutaconic acid can help to point out *MT-ATP6* mutations.

MATERIALS AND METHODS

Patients screening and case reports

The *MT-ATP6* gene was analyzed by CSGE or by sequencing of DNA obtained from blood or muscle samples of 550 patients that were referred to our laboratory after a suspect of mitochondrial disease. All samples were collected with informed consent of the patients and family members and the study was approved by the Ethics Review Committees of the involved Hospitals and of the Government of Aragón (CEICA 11/2010). These patients included individuals with MILS or NARP, in which we had previously ruled out the presence of the m.8993 and m.9176 mutations by PCR-RFLP. Many others suffered from other pathologies, such as optic neuropathies. Three of these patients presented interesting mutations.

The first patient (P1), a girl, is the first child born from healthy non-consanguineous parents. Familial antecedents were uneventful. The pregnancy was normal and the serology negative. The delivery was at 40 weeks by caesarean section with meconium-stained amniotic fluid. Since birth and due to respiratory depression, bradycardia and hypotonia, mechanic ventilation was applied. Clinical examination showed microcephaly, severe axial hypotonia, low deep tendon reflexes and pin cataract on the left eye. Computerized tomography scan and magnetic resonance imaging (MRI) showed cerebellum and brainstem atrophy and diffuse increased signal on cerebellar white matter. Motor and sensitive neuropathy was detected with electromyography and nerve conduction velocity. The respiratory problems were aggravated in the following days with severe bradycardia that

did not respond to reanimation procedures and lead her to death at 41 days of life. Necropsy studies confirmed severe atrophy of the cerebellum and brainstem. There was loss of granule and Purkinje cells and important astrocytosis of the cerebellar white matter. Clinical picture was of LS but ganglia were not affected on MRI or on the anatomopathologic study.

Lactate, pyruvate and alanine were elevated in blood. Urine organic acid analysis disclosed increased 3-methylglutaconic acid (34 mmol/mol creatinine; control range 5–15). In muscle, normalized respiratory complexes I+III (CI + III), II + III (CII + III) and IV (CIV) activities were not diminished. In the liver, CI + III was severely decreased, CII + III increased and CIV normal. PDH was normal as well (Supplementary Material, Table S1). Normal muscle CI + III and CII + III and elevated liver CII + III activities ruled out a CoQ deficit. Total and non-esterified carnitine levels in the muscle were 26 and 36%, respectively, of the lower limit for the control ranges (Supplementary Material, Table S1).

The second patient (P2) is a 38-year-old caucasian male who first came to our clinic complaining of a 4-year history of progressive visual loss. He was tentatively diagnosed of retinal ischemia 4 months prior to consultation. On examination, his best-corrected visual acuity was 20/80 in the right eye and 20/70 in the left eye. The anterior segments examination was within normal limits. The intraocular pressure was 12 mmHg in both eyes. Posterior segment evaluation showed the temporal half of the optic disc to be pale in both eyes. Visual evoked potentials showed a markedly increased latency in both eyes. Paracentral visual field defects were seen by the Goldmann visual field analysis. He was diagnosed as suffering an atypical LHON. His visual acuity and the anterior and posterior segment exam and visual fields were unchanged after four and a half years of oral multivitamin therapy on daily basis, especially B_6 and B_{12}. Family history was negative for visual loss or neurological disease.

The third patient (P3) is a male resulting from an uncomplicated pregnancy and delivery. He is the second child from non-consanguineous parents. Since birth he showed a mild motor delay. At 12 months, he was admitted to the hospital because of recurrent vomiting episodes and metabolic acidosis that persisted throughout his childhood. His height and weight remained steady at high percentile during development. He had learning difficulties at school. At the age of 7 years, an ophthalmologic evaluation revealed decreased visual acuity and mild bilateral macular pigmentary changes being diagnosed with pigmentary retinopathy. Currently, the patient is 16 years old and the most recent examination has revealed a mild ataxic gait, hypoactive reflexes and bilateral hypoacusia along with visual deficit. He has remained relatively stable for the last years. The laboratory tests, the screening for metabolic disorders including lactate and pyruvate levels in basal conditions, the thyroid and liver function, and the serum creatine kinase level have been repeatedly normal, and the karyotype was also normal. No lactate determination was recorded during any of the metabolic acidosis episodes in his pediatrics history. The electrophysiological study showed a subclinical sensory neuropathy and the brain MRI detects cerebellar vermis atrophy. His mother presented with progressive both unstable gait and bilateral sensorineural hearing loss since more than 15 years ago. She also presented bilateral concentric visual loss with a final diagnosis of retinitis

pigmentosa. Examination disclosed a proximal weakness of lower limbs. The laboratory tests, electrophysiogical studies and brain MRI are normal. The grandmother presented visual disturbances without a definitive diagnosis. The clinical phenotype of both patients (mother and son) was highly suggested of NARP syndrome. New sequence accession numbers: GenBank KJ742709-KJ742715.

Molecular-genetic analyses

The *MT-ATP6* gene was screened by CSGE and/or sequencing. The *ATP5G1*, *ATP5G2* and *ATP5G3* genes for the three isoforms of subunit c from the ATP synthase were screened by sequencing. The primers and conditions for these analyses and for the whole mtDNA sequencing are available upon request. The percentage of mutation was studied by the PCR-RFLP analysis (Supplementary Material, Table S2). For the hot-PCR, 2 μCi of $[\alpha^{-32}P]$ dCTP (3000 Ci/mmol) was added and one additional cycle was performed. The mtDNA content was measured by using protocols described elsewhere (52).

Bioinformatics explorations

The possibility of amplifying a nuclear sequence similar to the 1822 bp amplicon, between mtDNA positions 8018–9839, was checked in the mitochondrial pseudogenes database from mitomap (4). The 21 580 human, 3410 eukaryote and 1409 prokaryote p.MT-ATP6 sequences were obtained from GenBank (18 October 2013). The MutPred scores for particular amino acid substitutions were previously provided (6).

Modeling studies of p.MT-ATP6

The structure of *E. coli* subunit a (PDB 1C17) (53) was obtained with the RasMol2.6 program. The intramolecular interactions for the bacterial equivalent positions to p.MT-ATP6:G167 and p.MT-ATP6:S167 were obtained with Swiss-PDB-Viewer v.4.0.1. For this analysis, the *E. coli* equivalent position (histidine 245) in TMH5 was *in silico* mutated to glutamic.

Production, maintenance and functional investigations of transmitochondrial cell lines

To homogenize nuclear and environmental factors, we built transmitochondrial cell lines or cybrids with the osteosarcoma 143B rho^0 nuclear background using patient and control platelets (54). The genetic fingerprints of the rho^0 cell line and cybrids were performed with AmpFLSTR® Identifiler® PCR Amplification Kit (Life Technologies). These cybrids were grown in Dulbecco's modified eagle medium with no antibiotics and containing glucose (4.5 g/l), pyruvate (0.11 g/l) and fetal bovine serum (5%).

The analyses of oxygen consumption, ROS, SOD2 mRNA and ATP were performed in triplicate in three independent experiments, according to the previously described protocols (55). Mitochondrial ATP levels were measured using the CellTiter-Glow Luminiscent Cell Viability Assay (Promega) according to the manufacturer's instructions. Briefly, 20 000 cells/well were seeded 10–12 h before measurement. Then, cells were washed twice with PBS and incubated for 2 h in

record solution with 5 mM 2-deoxy-D-glucose plus 1 mM pyruvate (56). Cells were lysed, and lysates were incubated with the luciferin/luciferase reagents. Samples were measured using a NovoStar MBG Labtech microplate luminometer, and the results referred to the protein quantity.

The determination of the mitochondrial inner membrane potential was also done in triplicate in three independent experiments using Mito-ID Membrane Potential Detection Kit (Enzo Life Sciences).

Statistics analysis

The statistical package StatView 6.0 was used to perform all the statistics. Data for mean and standard deviation are presented. The unpaired two-tailed *t*-test was used to compare parameters. *P*-values < 0.05 were considered statistically significant.

SUPPLEMENTARY MATERIAL

Supplementary Material is available at *HMG* online.

ACKNOWLEDGEMENTS

FUNDING

REFERENCES

1. Thorburn, D.R. and Rahman, S. (1993) Mitochondrial DNA-Associated Leigh Syndrome and NARP. In Pagon, R.A., Adam, M.P., Ardinger, H.H., Bird, T.D., Dolan, C.R., Fong, C.T., Smith, R.J.H. and Stephens, K. (eds), *GeneReviews* [Internet], University of Washington, Seattle, WA: 1993–2014. 2003 October 30 [updated 2014 April 17] (www.ncbi.nlm.nih.gov/books/NBK1173/).

2. Schon, E.A., Santra, S., Pallotti, F. and Girvin, M.E. (2001) Pathogenesis of primary defects in mitochondrial ATP synthesis. *Semin. Cell Dev. Biol.*, **12**, 441–448.

3. Vives-Bauza, C., Yang, L. and Manfredi, G. (2007) Assay of mitochondrial ATP synthesis in animal cells and tissues. *Methods Cell Biol.*, **80**, 155–171.

4. Mishmar, D., Ruiz-Pesini, E., Brandon, M. and Wallace, D.C. (2004) Mitochondrial DNA-like sequences in the nucleus (NUMTs): insights into our African origins and the mechanism of foreign DNA integration. *Hum. Mutat.*, **23**, 125–133.

5. Giordano, C., Iommarini, L., Giordano, L., Maresca, A., Pisano, A., Valentino, M.L., Caporali, L., Liguori, R., Deceglie, S., Roberti, M. *et al.* (2014) Efficient mitochondrial biogenesis drives incomplete penetrance in Leber's hereditary optic neuropathy. *Brain*, **137**, 335–353.

6. Pereira, L., Soares, P., Radivojac, P., Li, B. and Samuels, D.C. (2011) Comparing phylogeny and the predicted pathogenicity of protein variations reveals equal purifying selection across the global human mtDNA diversity. *Am. J. Hum. Genet.*, **88**, 433–439.

7. Fillingame, R.H., Angevine, C.M. and Dmitriev, O.Y. (2002) Coupling proton movements to c-ring rotation in F(1)F(o) ATP synthase: aqueous access channels and helix rotations at the a-c interface. *Biochim. Biophys. Acta*, **1555**, 29–36.

8. King, M.P. and Attardi, G. (1989) Human cells lacking mtDNA: repopulation with exogenous mitochondria by complementation. *Science*, **246**, 500–503.

9. D'Aurelio, M., Vives-Bauza, C., Davidson, M.M. and Manfredi, G. (2010) Mitochondrial DNA background modifies the bioenergetics of NARP/MILS ATP6 mutant cells. *Hum. Mol Genet.*, **19**, 374–386.

10. Verny, C., Guegen, N., Desquiret, V., Chevrollier, A., Prundean, A., Dubas, F., Cassereau, J., Ferre, M., Amati-Bonneau, P., Bonneau, D. *et al.* (2011) Hereditary spastic paraplegia-like disorder due to a mitochondrial ATP6 gene point mutation. *Mitochondrion*, **11**, 70–75.

11. Synofzik, M., Schicks, J., Wilhelm, C., Bornemann, A. and Schols, L. (2012) Charcot-Marie-Tooth hereditary neuropathy due to a mitochondrial ATP6 mutation. *Eur. J. Neurol.*, **19**, e114–e116.

12. Childs, A.M., Hutchin, T., Pysden, K., Highet, L., Bamford, J., Livingston, J. and Crow, Y.J. (2007) Variable phenotype including Leigh syndrome with a 9185T>C mutation in the MTATP6 gene. *Neuropediatrics*, **38**, 313–316.

13. Angevine, C.M. and Fillingame, R.H. (2003) Aqueous access channels in subunit a of rotary ATP synthase. *J. Biol. Chem.*, **278**, 6066–6074.

14. Fillingame, R.H., Angevine, C.M. and Dmitriev, O.Y. (2003) Mechanics of coupling proton movements to c-ring rotation in ATP synthase. *FEBS Lett.*, **555**, 29–34.

15. Wang, Z., Hicks, D.B., Guffanti, A.A., Baldwin, K. and Krulwich, T.A. (2004) Replacement of amino acid sequence features of a- and c-subunits of ATP synthases of Alkaliphilic Bacillus with the Bacillus consensus sequence results in defective oxidative phosphorylation and non-fermentative growth at pH 10.5. *J. Biol. Chem.*, **279**, 26546–26554.

16. Cain, B.D. and Simoni, R.D. (1988) Interaction between Glu-219 and His-245 within the a subunit of F1F0-ATPase in Escherichia coli. *J. Biol. Chem.*, **263**, 6606–6612.

17. Cain, B.D. and Simoni, R.D. (1989) Proton translocation by the F1F0ATPase of Escherichia coli. Mutagenic analysis of the a subunit. *J. Biol. Chem.*, **264**, 3292–3300.

18. Hartzog, P.E. and Cain, B.D. (1994) Second-site suppressor mutations at glycine 218 and histidine 245 in the alpha subunit of F1F0 ATP synthase in Escherichia coli. *J. Biol. Chem.*, **269**, 32313–32317.

19. Howell, N., Herrnstadt, C., Shults, C. and Mackey, D.A. (2003) Low penetrance of the 14484 LHON mutation when it arises in a non-haplogroup J mtDNA background. *Am. J. Med. Genet. A*, **119A**, 147–151.

20. Tang, S., Wang, J., Zhang, V.W., Li, F.Y., Landsverk, M., Cui, H., Truong, C.K., Wang, G., Chen, L.C., Graham, B. *et al.* (2013) Transition to next generation analysis of the whole mitochondrial genome: a summary of molecular defects. *Hum. Mutat.*, **34**, 882–893.

21. Durham, S.E., Samuels, D.C., Cree, L.M. and Chinnery, P.F. (2007) Normal levels of wild-type mitochondrial DNA maintain cytochrome c oxidase activity for two pathogenic mitochondrial DNA mutations but not for m.3243A-->G. *Am. J. Hum. Genet.*, **81**, 189–195.

22. Zhang, D. and Vik, S.B. (2003) Close proximity of a cytoplasmic loop of subunit a with c subunits of the ATP synthase from Escherichia coli. *J. Biol. Chem.*, **278**, 12319–12324.

23. Zhang, D. and Vik, S.B. (2003) Helix packing in subunit a of the Escherichia coli ATP synthase as determined by chemical labeling and proteolysis of the cysteine-substituted protein. *Biochemistry*, **42**, 331–337.

24. Valiyaveetil, F.I. and Fillingame, R.H. (1997) On the role of Arg-210 and Glu-219 of subunit a in proton translocation by the Escherichia coli F0F1-ATP synthase. *J. Biol. Chem.*, **272**, 32635–32641.

25. Hatch, L.P., Cox, G.B. and Howitt, S.M. (1998) Glutamate residues at positions 219 and 252 in the a-subunit of the Escherichia coli ATP synthase are not functionally equivalent. *Biochim. Biophys. Acta*, **1363**, 217–223.

26. Kuo, P.H. and Nakamoto, R.K. (2000) Intragenic and intergenic suppression of the Escherichia coli ATP synthase subunit a mutation of Gly-213 to Asn: functional interactions between residues in the proton transport site. *Biochem. J.*, **347**(Pt 3), 797–805.

27. Angevine, C.M., Herold, K.A. and Fillingame, R.H. (2003) Aqueous access pathways in subunit a of rotary ATP synthase extend to both sides of the membrane. *Proc. Natl Acad. Sci. USA*, **100**, 13179–13183.

28. Jacobson, D.M. and Stone, E.M. (1991) Difficulty differentiating Leber's from dominant optic neuropathy in a patient with remote visual loss. *J. Clin. Neuroophthalmol.*, **11**, 152–157.

29. Borruat, F.X., Green, W.T., Graham, E.M., Sweeney, M.G., Morgan-Hughes, J.A. and Sanders, M.D. (1992) Late onset Leber's optic neuropathy: a case confused with ischaemic optic neuropathy. *Br. J. Ophthalmol.*, **76**, 571–573.

30. Cawley, N., Molloy, A., Cassidy, L. and Tubridy, N. (2010) Late-onset progressive visual loss in a man with unusual MRI findings: MS, Harding's, Leber's or Leber's Plus? *Ir. J. Med. Sci.*, **179**, 599–601.

31. Yen, M.Y., Wei, Y.H. and Liu, J.H. (1996) Stargardt's type maculopathy in a patient with 11778 Leber's optic neuropathy. *J. Neuroophthalmol.*, **16**, 120–123.

32. Tran, M., Bhargava, R. and MacDonald, I.M. (2001) Leber hereditary optic neuropathy, progressive visual loss, and multiple-sclerosis-like symptoms. *Am. J. Ophthalmol.*, **132**, 591–593.

33. Funalot, B., Reynier, P., Vighetto, A., Ranoux, D., Bonnefont, J.P., Godinot, C., Malthiery, Y. and Mas, J.L. (2002) Leigh-like encephalopathy complicating Leber's hereditary optic neuropathy. *Ann. Neurol.*, **52**, 374–377.

34. Baracca, A., Solaini, G., Sgarbi, G., Lenaz, G., Baruzzi, A., Schapira, A.H., Martinuzzi, A. and Carelli, V. (2005) Severe impairment of complex I-driven adenosine triphosphate synthesis in Leber hereditary optic neuropathy cybrids. *Arch. Neurol.*, **62**, 730–736.

35. Giordano, C., Montopoli, M., Perli, E., Orlandi, M., Fantin, M., Ross-Cisneros, F.N., Caparrotta, L., Martinuzzi, A., Ragazzi, E., Ghelli, A. *et al.* (2011) Oestrogens ameliorate mitochondrial dysfunction in Leber's hereditary optic neuropathy. *Brain*, **134**, 220–234.

36. Carrozzo, R., Rizza, T., Stringaro, A., Pierini, R., Mormone, E., Santorelli, F.M., Malorni, W. and Matarrese, P. (2004) Maternally-inherited Leigh syndrome-related mutations bolster mitochondrial-mediated apoptosis. *J. Neurochem.*, **90**, 490–501.

37. Geromel, V., Kadhom, N., Cebalos-Picot, I., Ouari, O., Polidori, A., Munnich, A., Rotig, A. and Rustin, P. (2001) Superoxide-induced massive apoptosis in cultured skin fibroblasts harboring the neurogenic ataxia retinitis pigmentosa (NARP) mutation in the ATPase-6 gene of the mitochondrial DNA. *Hum. Mol. Genet.*, **10**, 1221–1228.

38. Carelli, V. and Sadun, A.A. (2001) Optic neuropathy in Lhon and Leigh syndrome. *Ophthalmology*, **108**, 1172–1173.

39. Carelli, V., Ross-Cisneros, F.N. and Sadun, A.A. (2004) Mitochondrial dysfunction as a cause of optic neuropathies. *Prog. Retin. Eye Res.*, **23**, 53–89.

40. Lamminen, T., Majander, A., Juvonen, V., Wikstrom, M., Aula, P., Nikoskelainen, E. and Savontous, M.L. (1995) A mitochondrial mutation at nt 9101 in the ATP synthase 6 gene associated with deficient oxidative phosphorylation in a family with Leber hereditary optic neuroretinopathy. *Am. J. Hum. Genet.*, **56**, 1238–1240.

41. Shidara, K. and Wakakura, M. (2012) Leber's hereditary optic neuropathy with the 3434, 9011 mitochondrial DNA point mutation. *Jpn J. Ophthalmol.*, **56**, 175–180.

42. Majander, A., Lamminen, T., Juvonen, V., Aula, P., Nikoskelainen, E., Savontaus, M.L. and Wikstrom, M. (1997) Mutations in subunit 6 of the F1F0-ATP synthase cause two entirely different diseases. *FEBS Lett.*, **412**, 351–354.

43. Kazuno, A.A., Munakata, K., Tanaka, M., Kato, N. and Kato, T. (2008) Relationships between mitochondrial DNA subhaplogroups and intracellular calcium dynamics. *Mitochondrion*, **8**, 164–169.

44. Vanhoof, G., Goossens, F., De Meester, I., Hendriks, D. and Scharpe, S. (1995) Proline motifs in peptides and their biological processing. *FASEB J.*, **9**, 736–744.

45. Cordes, F.S., Bright, J.N. and Sansom, M.S. (2002) Proline-induced distortions of transmembrane helices. *J. Mol. Biol.*, **323**, 951–960.

46. Lopez-Gallardo, E., Solano, A., Herrero-Martin, M.D., Martinez-Romero, I., Castano-Perez, M.D., Andreu, A.L., Herrera, A., Lopez-Perez, M.J., Ruiz-Pesini, E. and Montoya, J. (2009) NARP syndrome in a patient harbouring an insertion in the MT-ATP6 gene that results in a truncated protein. *J. Med. Genet.*, **46**, 64–67.

47. Blanco-Grau, A., Bonaventura-Ibars, I., Coll-Canti, J., Melia, M.J., Martinez, R., Martinez-Gallo, M., Andreu, A.L., Pinos, T. and Garcia-Arumi, E. (2013) Identification and biochemical characterization of the novel mutation m.8839G>C in the mitochondrial ATP6 gene associated with NARP syndrome. *Genes Brain Behav.*, **12**, 812–820.

48. Duno, M., Wibrand, F., Baggesen, K., Rosenberg, T., Kjaer, N. and Frederiksen, A.L. (2013) A novel mitochondrial mutation m.8989G>C associated with neuropathy, ataxia, retinitis pigmentosa - the NARP syndrome. *Gene*, **515**, 372–375.

49. Pitceathly, R.D., Murphy, S.M., Cottenie, E., Chalasani, A., Sweeney, M.G., Woodward, C., Mudanohwo, E.E., Hargreaves, I., Heales, S., Land, J. *et al.* (2012) Genetic dysfunction of MT-ATP6 causes axonal Charcot-Marie-Tooth disease. *Neurology*, **79**, 1145–1154.

50. Aure, K., Dubourg, O., Jardel, C., Clarysse, L., Sternberg, D., Fournier, E., Laforet, P., Streichenberger, N., Petiot, P., Gervais-Bernard, H. *et al.* (2013) Episodic weakness due to mitochondrial DNA MT-ATP6/8 mutations. *Neurology*, **81**, 1810–1818.

51. Ware, S.M., El-Hassan, N., Kahler, S.G., Zhang, Q., Ma, Y.W., Miller, E., Wong, B., Spicer, R.L., Craigen, W.J., Kozel, B.A. *et al.* (2009) Infantile cardiomyopathy caused by a mutation in the overlapping region of mitochondrial ATPase 6 and 8 genes. *J. Med. Genet.*, **46**, 308–314.

52. Marcuello, A., Gonzalez-Alonso, J., Calbet, J.A., Damsgaard, R., Lopez-Perez, M.J. and Diez-Sanchez, C. (2005) Skeletal muscle mitochondrial DNA content in exercising humans. *J. Appl. Physiol. (1985)*, **99**, 1372–1377.

53. Rastogi, V.K. and Girvin, M.E. (1999) Structural changes linked to proton translocation by subunit c of the ATP synthase. *Nature*, **402**, 263–268.

54. Chomyn, A., Lai, S.T., Shakeley, R., Bresolin, N., Scarlato, G. and Attardi, G. (1994) Platelet-mediated transformation of mtDNA-less human cells: analysis of phenotypic variability among clones from normal individuals—and complementation behavior of the tRNALys mutation causing myoclonic epilepsy and ragged red fibers. *Am. J. Hum. Genet.*, **54**, 966–974.

55. Gomez-Duran, A., Pacheu-Grau, D., Lopez-Gallardo, E., Diez-Sanchez, C., Montoya, J., Lopez-Perez, M.J. and Ruiz-Pesini, E. (2010) Unmasking the causes of multifactorial disorders: OXPHOS differences between mitochondrial haplogroups. *Hum. Mol. Genet.*, **19**, 3343–3353.

56. Gong, S., Peng, Y., Jiang, P., Wang, M., Fan, M., Wang, X., Zhou, H., Li, H., Yan, Q., Huang, T. *et al.* (2014) A deafness-associated tRNAHis mutation alters the mitochondridal function, ROS production and membrane potential. *Nucleic Acids Res.*, **42**, 8039–8048.